



Wang, L., Zhang, W., Na, J., Li, G., & Su, S. (2016). Robust repetitive control of three-phase inverter system using high order internal model. In *Chinese Control Conference, CCC* (pp. 8544-8549). [7554722] (Proceedings of the Chinese Control Conference). IEEE Computer Society. <https://doi.org/10.1109/ChiCC.2016.7554722>

Peer reviewed version

Link to published version (if available):
[10.1109/ChiCC.2016.7554722](https://doi.org/10.1109/ChiCC.2016.7554722)

[Link to publication record in Explore Bristol Research](#)
PDF-document

This is the author accepted manuscript (AAM). The final published version (version of record) is available online via IEEE at <http://ieeexplore.ieee.org/document/7554722/> . Please refer to any applicable terms of use of the publisher.

University of Bristol - Explore Bristol Research

General rights

This document is made available in accordance with publisher policies. Please cite only the published version using the reference above. Full terms of use are available:
<http://www.bristol.ac.uk/red/research-policy/pure/user-guides/ebr-terms/>

Robust Repetitive Control of Three-phase Inverter System Using High Order Internal Model

Ligang Wang¹, Wenbing Zhang¹, Jing Na^{*1}, Guang Li², Shi Su³

1. Faculty of Mechanical & Electrical Engineering, Kunming University of Science & Technology, Kunming, 650500, P.R. China

E-mail: najing25@163.com

2. School of Engineering and Material Sciences, Queen Mary, University of London, UK

3. Yunnan Power Grid Electric Power Research Institute Co., Ltd., Kunming, 650217, P.R. China

Abstract: In order to improve the static and dynamic responses of three-phase grid-connected inverter systems, this paper proposes a composite control consisting of a PI control and a repetitive control. This method can be used to reject the periodic harmonic signals, and thus improve the converter output performance. A high-order repetitive controller is adopted to further improve the robustness against the uncertainties in the period of signals. The main contribution of this paper is to analyze and compare the robustness of first-order repetitive control and high-order repetitive control against modeling error and frequency variation. Finally, comparative simulations based on a circuit level inverter model are conducted to show that high-order repetitive control can reduce the net current harmonics of the three-phase inverter system when there are period uncertainties, and thus obtain better steady-state and dynamic responses.

Key Words: Repetitive control, high-order internal model, three-phase inverter systems, robustness analysis.

1 Introduction

In sustainable energy and power generation systems, e.g. photovoltaic and wind power generation, the grid-connected inverter is one of the central components. However, the inverter is usually subject to non-linear loads and external disturbances, which will generate harmonics and affect the whole power grid. Due to the imposed strict requirements on the harmonic contents of current feeding into the grid [1], it is particularly important to control the current output of the inverter. This issue can be addressed either by designing filters to filter out harmonics or by using advanced control algorithms. It is noted that the filters with fixed parameters may also be sensitive to system variations.

For control design of inverters, considering the fact that the power electronic systems are generally dealing with periodic signals, repetitive control (RC) [2] can be used, which can suppress periodic disturbances. The essential feature is that the constructed internal model has infinite gains at all multiples of the basic frequency, and thus any signal with those periods can be perfectly rejected or tracked provided that the overall closed-loop system is stable [3]. Thus, RC has been widely used in the power electronics systems [4-9]. It is noted that RC is usually designed, assuming that the period of reference or disturbance signals is precisely known. However, in the distributed power generation systems, the grid frequency may be fluctuant.

In order to improve the performance of RC, two potential methods were proposed: the first one is to add a frequency observer in the system [10-12]. Although this method can obtain a fairly good result, it will bring the stability analysis from a linear time-invariant framework into a linear time-varying one. The second method is to use a high order internal model, where multiple repetitive loops are adopted; this leads to high order repetitive control (HORC) [13-15].

The aim of this paper is to propose a robust repetitive control scheme for a three-phase grid-connected inverter system to reject output current harmonics and improve the quality of electric energy. The designed current controller is composed of a PI controller and a repetitive controller. The PI controller is designed to stabilize the closed-loop system, and the repetitive controller is used to regulate the inverter output current to reduce total harmonic distortion (THD) of the net current. We also compare the essential features of the first order repetitive control (FORC) and HORC, and analyze their performance and robustness against modeling errors and signal's frequency variation. In comparison to [4-8, 16], this paper quantitatively studies the robust stability of the closed-loop system with RC and HORC. This can be considered as a further development of our previous work [17, 18]. We find that the robustness of HORC against period variations is better than FORC. However, the robustness of HORC with other modeling uncertainties may degrade as the order of RC is increased. Finally, these theoretical analyses are verified via simulations based on a circuit level inverter system built in Matlab/Simulink.

2 Problem Formulation

As one of core components in the distributed power generation system, the grid-connected inverter determines the quality of the current feeding into the grid. Fig. 1 presents the topology of a three-phase grid-connected inverter.

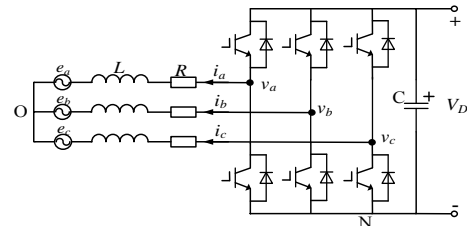


Fig. 1 Topology of three-phase grid-connected inverter.

In Fig.1, V_D is the DC bus voltage, C is the DC bus capacitor, e_a, e_b, e_c are the grid voltages, L and R denote

This work is supported by National Natural Science Foundation (NSFC) of China under Grants 61203066, 61573174, and Basic Research Planning Project of Yunnan Province under Grant 2013FB028.

* Corresponding author: Jing Na (Email: najing25@163.com)

the filter inductor and resistance, v_a, v_b, v_c and i_a, i_b, i_c are the inverter output voltages and currents, respectively.

As the induced current harmonics may degrade the power quality, a controller should be used to suppress harmonics and to reduce the distortion of current. The current and voltage should be regulated in the same phase and frequency, so that a PLL(Phase Locked Loop) is introduced. Fig. 2 depicts the architecture of the designed control system.

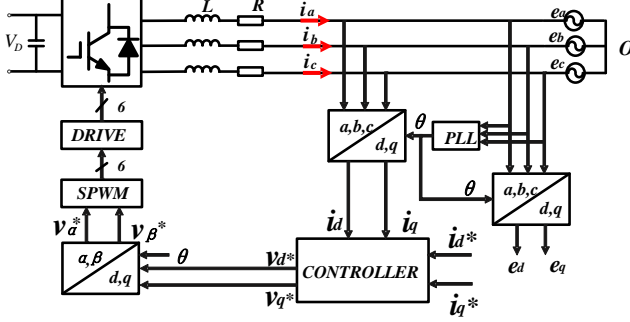


Fig. 2 Architecture of the overall control system.

For d - q coordinate system, the mathematical model of Fig. 2 is given by

$$\begin{cases} v_d = e_d + i_d R + L \frac{di_d}{dt} - \omega L i_q \\ v_q = e_q + i_q R + L \frac{di_q}{dt} + \omega L i_d \end{cases} \quad (1)$$

where i_d, i_q are obtained by Clark and Park transform of i_a, i_b, i_c . v_d, v_q and e_d, e_q can be obtained based on v_a, v_b, v_c and e_a, e_b, e_c . ω is the network frequency, i.e. 50Hz.

The objective is to design appropriate controllers to manipulate v_d, v_q such that the output current i_d, i_q can track ideal reference with small THD. We take d axis as an example to present the control design. It is shown that there are coupling effects in Eq. (1). Moreover, the inverter bridges have amplification ratios from the control signal to the output voltage, which create a fair response time. Taking into account these factors, the transfer function of the inverter can be approximated as

$$P(s) = \frac{i(s)}{v(s) - e(s)} = \frac{K_{PWM}}{1.5\tau_s s + 1} \cdot \frac{1}{Ls + R} \quad (2)$$

where K_{PWM} is the gain of PWM inverter, τ_s is the PWM inverter switching period.

Since the jamming signal in the power electronic system is periodic, a particular control structure shown in Fig.3 is used.

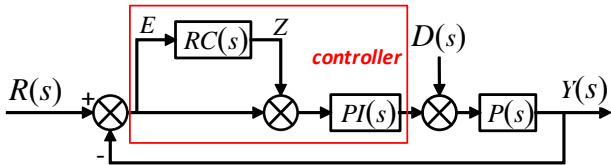


Fig. 3 Overall control structure.

This control system in Fig.3 consists of a RC controller and a PI controller. PI Controller is designed to stabilize the closed-loop system, whose parameters can be tuned as [19]. This paper will focus on the design of repetitive control (FORC and HORC) and comparisons.

3 First Order Repetitive Control (FORC)

3.1 Repetitive Control Structure

Repetitive control is designed based on an internal model (IM) as shown in Fig.4, which can learn a signal of the period T and duplicate it even if the input signal of this model is set to zero. From the frequency point of view, this internal model introduces infinite gain (without filter $H(s)$) at the specific frequencies $\omega = 2n\pi/T$ rad/s for $\forall n \in N^+$. Then according to the Internal Model Principle (IMP)[20], zero- error tracking or rejection of signals with such frequencies can be guaranteed if the closed-loop system is stable [9].

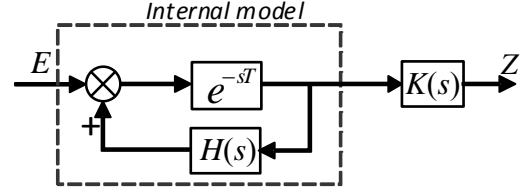


Fig. 4 Block diagram of FORC.

The low-pass filter $H(s)$ in Fig.4 is used to improve the robustness although it may reduce the gains in these specific frequencies [4-8, 16]. In this paper, $H(s)$ is set as a second order Butterworth filter. The compensator $K(s)$ is used to retain the system stability. Thus the transfer function of RC is described by

$$RC(s) = \frac{Z(s)}{E(s)} = \frac{e^{-sT}}{1 - H(s)e^{-sT}} \cdot K(s) \quad (3)$$

3.2 Stability and Performance Analysis

The following conditions should be fulfilled to guarantee the stability of the closed-loop system.

Proposition 1 [4-8, 16]: The closed-loop system in Fig. 3 with RC in Fig. 4 is stable if the following conditions are fulfilled:

- 1) The closed-loop system without RC is stable, i.e. $T_0(s) = PI(s)P(s)/(1 + PI(s)P(s))$ is stable.
- 2) $\|H(s)\|_\infty \leq 1$.
- 3) $\|(K(s)T_0(s) - H(s))e^{-sT}\|_\infty = \|K(s)T_0(s) - H(s)\|_\infty \leq 1$.

Proof: We refer to [4-8, 16] for a detailed proof, which will not be provided due to the limited space.

PI control is designed to fulfill condition 1), a low-pass filter $H(s)$ is used to fulfill condition 2), $K(s)$ can be designed to satisfy condition 3). For any minimum-phase plant $P(s)$, a constructive design of $K(s)$ is given as [17]

$$K(s) = k_r H(s) / T_0(s) \quad (4)$$

where k_r is a constant.

Substituting (4) into Proposition 1, we have:

Corollary 1: The closed-loop control system in Fig.3 with minimum-phase $P(s)$ and compensator (4) is stable if the following conditions are fulfilled:

- 1) $\|H(s)\|_\infty \leq 1$.
- 2) k_r is a constant fulfilling $|k_r - 1| \leq 1 / \|H(s)\|_\infty$.

In spite of stability, the tracking performance of periodic signals can be guaranteed by verifying the open-loop gain of

the RC system in Fig.3, which can be obtained from (3) and (4). It has been shown in [4-8, 16] that the gains of this system tend to very high values at the multiples of the input signal frequency $\omega = 2n\pi/T$, thus the output $Y(s)$ can follow the reference $R(s)$. Moreover, to show the harmonic rejection, the transfer function from $E(s)$ to $D(s)$ can be obtained as

$$\frac{E}{D} = -\frac{P(s)}{1 + (1 + RC)PI(s)P(s)} = -\frac{1 - H(s)e^{-sT}}{1 + PI(s)P(s)} \cdot \frac{P(s)}{1 + (K(s)T_0(s) - H(s))e^{-sT}} \quad (5)$$

It can be found that if the filter $H(s)$ has gains close to 1, the gain of (5) are close to zero at $\omega = 2n\pi/T$. Thus, the effect of the disturbances $D(s)$ can be eliminated.

3.3 Robustness Analysis

We will study the robust stability of the closed-loop system shown in Fig.3 against modeling uncertainties. We denote $P(s)$ as the plant, and $P_n(s)$ as the nominal model, which is used to design $K(s)$. We rewrite $P(s) = P_n(s)(1 + \delta P(s))$, where $\delta P(s)$ denotes the multiplicative errors [21], which fulfills $|\delta P(s)| \leq \overline{\delta P}(s)$, $\forall s = j\omega, \omega > 0$ with $\overline{\delta P}(s)$ being the upper error bound. Then we have

Proposition 2: The closed-loop system in Fig.3 with RC in Fig. 4 is robust stable if the following conditions hold:

- 1) The conditions in Proposition 1 are fulfilled;
- 2) The multiplicative uncertainties are bounded by

$$\overline{\delta P}(s) \Big|_{s=j\omega} < \left| 1 + \frac{1 - H(j\omega)e^{-j\omega T}}{(1 - He^{-j\omega T})PI(j\omega)P(j\omega) + k_r He^{-j\omega T}(1 + PI(j\omega)P(j\omega))} \right|$$

Proof: When there are modeling uncertainties $\delta P(s)$, the compensator $K(s)$ can only be designed via $P_n(s)$. Then the closed-loop system characteristic equation is written as $1 + (1 + RC(s))PI(s)P(s) = 1 + (1 + RC(s))PI(s)P_n(s)(1 + \delta P(s))$

$$= [1 + (1 + RC(s))PI(s)P_n(s)] + (1 + RC(s))PI(s)P_n(s)\delta P(s) = 0 \quad (6)$$

The first part of (6) is indeed the characteristic equation of the nominal control system of Fig. 3. Thus, the conditions of Proposition 1 are sufficient to retain its stability. The second part defines the effect of $\delta P(s)$ on the closed-loop stability. As explained in [21], the additional stability conditions for (6) is that, for all frequencies ($\forall s = j\omega, \omega > 0$) and for all plants in the family $|\delta P(s)| \leq \overline{\delta P}(s)$, the distance between the curve of $(1 + RC(s))PI(s)P_n(s)$ and the point $(-1, 0)$ in the Nyquist plot (i.e. $|1 + (1 + RC(s))PI(s)P_n(s)|_{s=j\omega}$) is larger than $|(1 + RC(s))PI(s)P_n(s)\delta P(s)|_{s=j\omega}$. Thus the maximum bound of allowable multiplicative error $|\delta P(s)|$ between the nominal model $P_n(s)$ and the actual system $P(s)$ is given by the following constraint:

$$\begin{aligned} |\delta P(s)| &< \frac{|1 + (1 + RC(s))PI(s)P_n(s)|}{|(1 + RC(s))PI(s)P_n(s)|} \Big|_{s=j\omega} \\ &= \left| 1 + \frac{1 - He^{-j\omega T}}{(1 - He^{-j\omega T})PI \cdot P + k_r He^{-j\omega T}(1 + PI \cdot P)} \right| \end{aligned} \quad (7)$$

Denote $dP(j\omega) = \left| 1 + \frac{1 - He^{-j\omega T}}{(1 - He^{-j\omega T})PIP + k_r He^{-j\omega T}(1 + PIP)} \right|$, then

system (6) is robust stable under the following condition

$$|\delta P(s)| = \frac{|P(s) - P_n(s)|}{|P_n(s)|} \leq \overline{\delta P}(s) < dP(s), \forall s = j\omega, \omega > 0 \quad (8)$$

Remark 1: According to (7), the robustness bound $dP(s)$ depends on the low-pass filter $H(s)$ and the constant k_r . A low cutoff frequency ω_c can improve the robustness, but may reduce the closed-loop bandwidth and thus the tracking and rejection performance. Moreover, a large k_r can lead to smaller robustness bound but high open-loop gain, which can improve the control response.

4 High Order Repetitive Control (HORC)

Although FORC in Fig.4 is easy to implement, its performance may degrade when the period T of reference or disturbance has uncertainties, i.e. it is sensitive to the variation in the period of signals. In order to tackle these disadvantages, high order repetitive control (HORC) was proposed in [13-15] as Fig. 8.

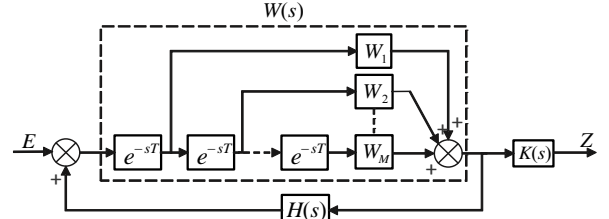


Fig. 5 Block diagram of HORC.

In Fig.8, $W(s)$ is a weighted sum function of repetitive loops. Thus, the transfer function of HORC can be written as

$$HORC(s) = \frac{W(s)K(s)}{1 - W(s)H(s)} \quad (9)$$

It is shown that HORC uses a multiple loop internal model, which replaces the delay e^{-sT} by a weighted sum function of several delays given as follows:

$$W(s) = \sum_{m=1}^M W_m e^{-msT} \quad (10)$$

where M is the number of delays, i.e. the order of RC loop.

Similar to FORC, the gains of HORC are infinite at the multiples of the input signal frequency. In particular, the gain of Eq.(9) will tend to infinity if $W(s)H(s) = 1$. As shown in [13], we substitute $s = jk2\pi/T$ into (10) and have

$$W(jk2\pi/T) = \sum_{m=1}^M W_m e^{-jmk2\pi} = \sum_{m=1}^M W_m = 1 \quad (11)$$

It is noted that for $M = 1$, $W_1 = 1$, Eq. (9) is reduced to FORC. For the case when $M > 1$, we need to determine the weight parameters W_m . Following the idea of [13], we can make the first order derivative of $W(s)$ with respect to T as zero at the specific frequency. This imposes the condition

$$\frac{\partial W(s = jk2\pi/T)}{\partial T} = \sum_{m=1}^M -W_m m jk2\pi/T = 0 \quad (12)$$

According to (12), the following equation is true

$$\sum_{m=1}^M W_m m = 0 \quad (13)$$

As shown in [13], to further decrease the sensitivity for period-time variations by using weight parameters of HORC, we can make $(M-1)$ -th derivatives equal to zero, so that

$$\sum_{m=1}^M W_m m^{(M-1)} = 0 \quad (14)$$

The weight parameters can be calculated based on Eqs.(11)~(14). For example, when $M=2$ and 3, we can set $W_1 = 2, W_2 = -1$ and $W_1 = 3, W_2 = -3, W_3 = 1$, respectively.

4.1 Stability and Performance Analysis

Proposition 3: The closed-loop system in Fig. 3 with HORC in Fig.5 is stable if the following conditions hold:

- 1) The closed-loop system without HORC loop is stable, i.e. $T_0(s) = PI(s)P(s)/(1 + PI(s)P(s))$ is stable.
- 2) $\|H(s)\|_\infty \leq 1$.
- 3) $\|(K(s)T_0(s) - H(s))W(s)\|_\infty \leq 1$.

Proof: The proof is similar to that of Proposition 1 by replacing e^{-sT} with $W(s)$.

For any minimum-phase $P(s)$, we design $K(s)$ as

$$K(s) = k_r H(s) / T_0(s) \quad (15)$$

Corollary 2: For stable, minimum-phase plant $P(s)$, the closed-loop control system shown in Fig.3 with HORC in Fig.5 is stable if the following conditions are true:

- 1) $\|H(s)\|_\infty \leq 1$.
- 2) k_r is a constant fulfilling $|k_r - 1| \leq 1 / \|H(s)W(s)\|_\infty$.

The tracking and disturbance rejection performance of HORC will be examined by calculating the open-loop gain of control system with HORC (9) and compensator (15). Fig. 6 shows the open loop gains of 1, 2, 3th-order RC (i.e. $M=1, 2, 3$) with $k_r = 1.2$, $H(s)=1$. As shown in Fig.6, the gains of all RCs all tend to very high values at the specific frequencies. In particular, the gains with HORC are higher than that of FORC. Thus, according to the internal model principle, precise reference tracking response can be guaranteed with both FORC and HORC.

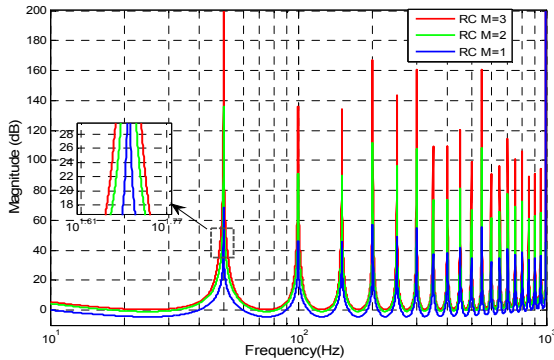


Fig. 6 Open loop gains of 1, 2, 3th order RC.

Moreover, the disturbance rejection of HORC can be shown by checking the transfer function from $E(s)$ to $D(s)$ as

$$\frac{E(s)}{D(s)} = -\frac{1 - H(s)W(s)}{1 + PI(s)P(s)} \frac{P(s)}{1 + (k_r - 1)H(s)W(s)} \quad (16)$$

It is known that $W(s) = \sum_{m=1}^M W_m e^{-msT} = 1$ holds at

frequencies $f = (n/T)\text{Hz}, n \in \mathbb{Z}$, and the gain of $H(s)$ is close to one, thus the gains of (16) are close to zero at these frequencies, so that the effect of the disturbances $D(s)$ is eliminated.

4.2 Robustness Analysis

We will analyze the robust stability of HORC when the system is subject to uncertainties in the plant model. In this case, only the nominal model $P_n(s)$ can be used to design $K(s)$. Similar to Section 3.3, the following Proposition 4 provides the robust stability conditions for the closed-loop system with HORC.

Proposition 4: The closed-loop control system in Fig. 3 with HORC is robust stable if the following conditions hold:

- 1) The conditions in Proposition 3 are satisfied;
- 2) The multiplicative uncertainties are bounded by

$$\left| \frac{\delta P(s)}{P(s)} \right|_{s=j\omega} < \left| 1 + \frac{1 - WH}{(1 - WH)PIP + k_r WH(1 + PIP)} \right|, \forall \omega > 0$$

Proof: The proof of Proposition 4 is similar to that of Proposition 2, and thus will not be repeated again.

5 Comparison of FORC and HORC

This section will compare the robust stability of FORC and HORC when the system has uncertainties $\delta P(s)$ in the plant model and in the period T of reference or disturbance signals.

Robustness Against Modeling Error

From Proposition 2 and Proposition 4, one can claim that the robustness bounds $dP(s)$ of FORC and HORC all depend on the cutoff frequency ω_c of low-pass filter $H(s)$ and the constant k_r . In general, the robustness can be improved with smaller ω_c and k_r , although the tracking and disturbance attenuation response are reduced due to the reduction in the open loop gain as shown in Fig. 6. Thus, it will be interesting to compare their performances.

For this purpose, it is noted that in HORC, the multiple delay loops $W(s) = \sum_{m=1}^M W_m e^{-msT}$ is used to replace the single

delay loop e^{-sT} . The use of weight gain parameters W_m (possibly larger than 1) in (10) can lead to smaller robust stability bounds in comparison to (7), which means that the robustness of HORC is weaker than that of FORC, when the system is subject to modeling error $\delta P(s)$. To show this analysis, we plot the robust bounds $dP(s)$ of FORC and 3-order RC with different k_r and ω_c , where the realistic

system $P(s) = \frac{1.8}{2.5 \times 10^{-6}s^2 + 3.8 \times 10^{-2}s + 0.1}$ and its nominal

model $P_n(s) = \frac{1}{4.5 \times 10^{-6}s^2 + 3.0015 \times 10^{-2}s + 0.1}$ are used.

Figs.7-8 depict the frequency response of the modeling error $\delta P(s)$ and the robust stability bound $dP(s)$ with different k_r and ω_c for the 1, 3 order RC, respectively. It is shown that a smaller control gain k_r and a lower cutoff

frequency ω_c give better robustness bounds (e.g. $k_r = 0.8$, $f_c = 500$ Hz), while larger k_r and ω_c can trigger instability (e.g. $k_r = 1.6$, $f_c = 1000$ Hz) under modeling errors.

Moreover, it is also shown that with same modeling error and parameters k_r, f_c , the robustness of 3-order RC is worse than that of 1-order RC. Similar conclusion can be drawn by comparing the 2-order RC with 3-order RC, that is the robust bounds of HRC against the modeling errors $\delta P(s)$ may degrade as the order M of the internal model increases. This may be due to the fact that more delay elements are adopted for HRC, which are sensitive to modeling uncertainties.

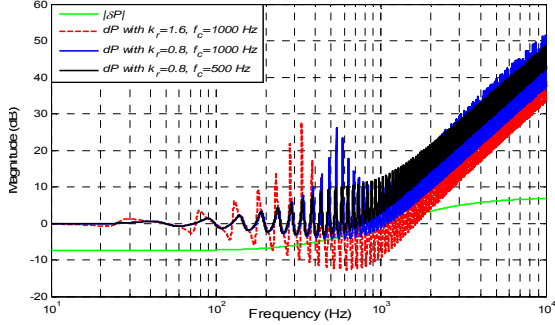


Fig. 7 Robust stability of FORC with different k_r and f_c .

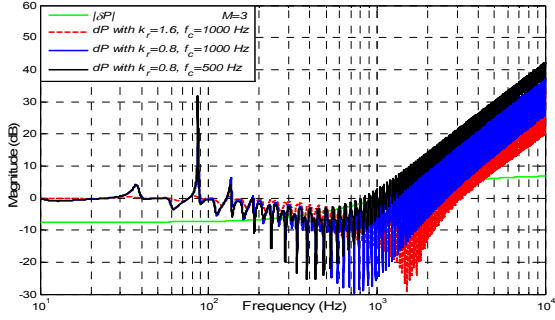


Fig. 8 Robust stability of 3-order RC with different k_r, f_c .

Robustness Against Period Fluctuation

The motivation for using HRC is to allow for potential fluctuations in the period T of reference to be tracked or disturbances to be rejected. This allows us to analyze its robustness from another perspective as in [13].

When the period of the reference or disturbance is not known exactly or cannot be measured accurately, we denote that the period has a multiplicative error δT (i.e. the period time $T(1+\delta T)$ is used in the design of RC). Then, the transfer function (9) for the periodic signal generator with $H(s) = 1$ and $s = jk2\pi/T$ can be given as

$$HRC(jk2\pi/T) = \frac{K(jk2\pi/T) \sum_{m=1}^M W_m e^{-mjk2\pi(1+\delta T)}}{1 - \sum_{m=1}^M W_m e^{-mjk2\pi(1+\delta T)}} \quad (17)$$

The magnitude of (17) for the first harmonic ($k = 1$) is plotted as a function of the perturbation δT in Fig.9. From Fig. 9, we can find that for a perturbation of 1.5%, the gain drops to 20dB for FORC. However, the gains of HRCs are greater than that of FORC. This means that the robustness against period error can be improved via HRC. This feature is even more pronounced for harmonics.

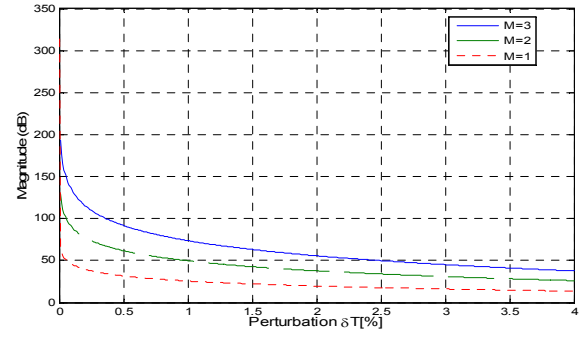


Fig. 9 Magnitude of (17) with $H(s) = 1$ for 1, 2, 3-order RC under the period perturbation δT (From 0% to 4%).

6 Simulations Results

In this section, simulation results based on a three phase inverter (Fig.1) emulated via SimPowerSystems toolbox in Matlab/Simulink are presented to validate the effectiveness of the proposed algorithms. The simulations are conducted in circuit level and thus are more realistic than the transfer function only. Thus, the modeling errors are unavoidable in these case studies. The nominal system parameters are given as: the phase to ground voltage $e = 220$ V, DC bus voltage $V_d = 800$ V; switching frequency $f_s = 10$ kHz, filter parameters are $L = 30$ mH, $R = 0.1 \Omega$, $f_c = 2500$ Hz. The harmonics rejection responses of the currents feeding into the grid are compared for FORC and HRC. We use FFT analysis tool in Simulink to get the total harmonic distortion (THD).

To compare the control performance and robustness against the error in the period, the frequency of the grid voltage is set as 49.9 Hz, and the 3th (10%) and 5th (5%) negative sequence harmonics are also added at the same time. We will compare the THD for three cases: PI controller, PI controller plus FORC, and PI controller plus 3-order RC. Simulation results are shown in Fig.10-Fig.12.

As shown in the figures, the THD of PI control is 2.34%, and it can be reduced to 1.8% when the FORC is applied. However, the 3th and 5th harmonics are still significant due to the uncertainty in the frequency. When the 3-order RC is adopted, the THD can be reduced to 1.03%, which is better than another two cases. In particular, the high order harmonics are significantly eliminated via HRC. These simulation results show that HRC performs better than FORC with respect to the robustness against to the errors in the period of the reference or disturbances.

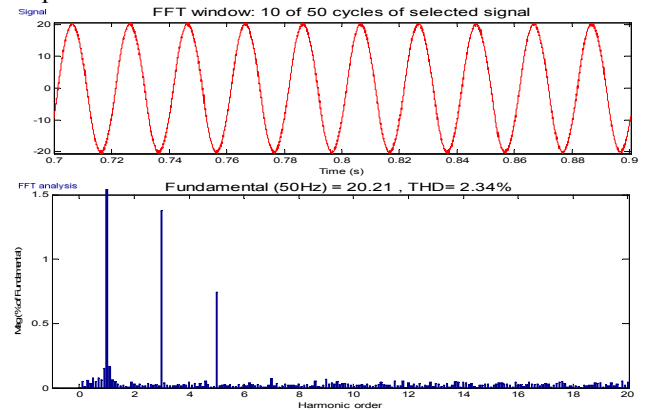


Fig. 10 Response of grid current i_d and its THD without RC at 49.9 Hz.

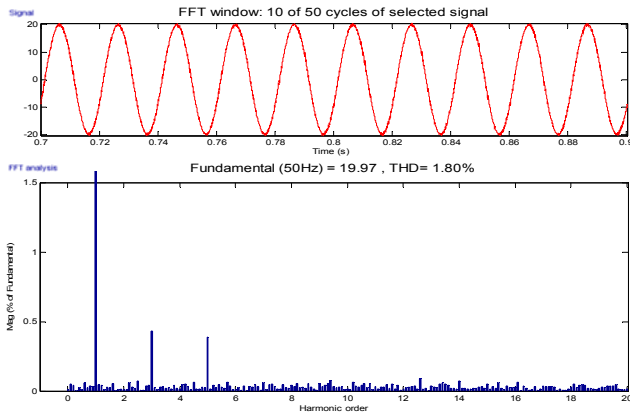


Fig. 11 Response of grid current i_a and its THD with first-order RC at 49.9 Hz.

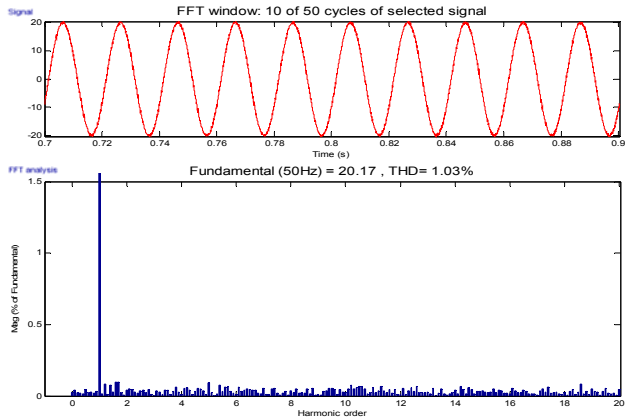


Fig. 12 Response of grid current i_a and its THD with third-order RC at 49.9 Hz.

7 Conclusions

In this paper, we incorporated the repetitive control into PI control to address harmonic rejection of a three-phase grid-connected inverter, where the frequency of grid voltage has small fluctuations. The main contribution is that we propose a systematic method to study the robustness of repetitive control schemes. Moreover, we also compare the performance and robustness of first order repetitive control (FORC) and high-order repetitive control (HORC) against to uncertainties in the plant model and signal periods. Circuit level simulations are also conducted to validate the analysis. It reveals that the HORC with multiple delay loops can enhance the robustness against the fluctuations in the periods, while its robustness to other modeling uncertainties may be deteriorated. Thus, the order of RC, the cutoff frequency and gain used in the control should be chosen as a tradeoff between performance and robustness.

References

- [1] R. Redl, P. Tenti, and J. Wyk, "Power electronics' polluting effects," *Spectrum, IEEE*, vol. 34, pp. 32-39, 1997.
- [2] M. Tomizuka, T.-C. Tsao, and K.-K. Chew, "Analysis and synthesis of discrete-time repetitive controllers," *Journal of Dynamic Systems, Measurement, and Control*, vol. 111, pp. 353-358, 1989.
- [3] J. Na, R. Costa-Castelló, R. Griño, and X. Ren, "Discrete-time repetitive controller for time-delay systems with disturbance observer," *Asian Journal of Control*, vol. 14, pp. 1340-1354, 2012.
- [4] R. Griño, R. Cardoner, R. Costa-Castelló, and E. Fossas, "Digital Repetitive Control Of A Three-Phase Four-Wire Shunt Active Filter," *Industrial Electronics IEEE Transactions on*, vol. 54, pp. 1495-1503, 2007.
- [5] R. Costa-Castelló, R. Griño, and E. Fossas, "Odd-harmonic digital repetitive control of a single-phase current active filter," *Power Electronics, IEEE Transactions on*, vol. 19, pp. 1060-1068, 2004.
- [6] R. Costa-Castelló, J. Nebot, and R. Griño, "Demonstration of the internal model principle by digital repetitive control of an educational laboratory plant," *Education, IEEE Transactions on*, vol. 48, pp. 73-80, 2005.
- [7] G. A. Ramos, R. Costa-Castelló, J. M. Olm, and R. Cardoner, "Robust high-order repetitive control of an active filter using an odd-harmonic internal model," in *Industrial Electronics (ISIE), 2010 IEEE International Symposium on, Bari, Italy, 2010*, pp. 1040-1045.
- [8] G. Weiss, Q. Zhong, and T. Green, "H-infinity repetitive control of dc-ac converters in microgrids," *IEEE Transactions on, Power Electronics*, vol. 19, pp. 567-567, 2004.
- [9] K. Zhou and D. Wang, "Digital repetitive learning controller for three-phase CVCF PWM inverter," *IEEE Transactions on Industrial Electronics*, vol. 48, pp. 820-830, 2001.
- [10] R. D. Hanson and T.-C. Tsao, "Periodic sampling interval repetitive control and its application to variable spindle speed noncircular turning process," *Journal of Dynamic systems, Measurement, and control*, vol. 122, pp. 560-566, 2000.
- [11] J. M. Olm, G. A. Ramos, and R. Costa-Castelló, "Odd-harmonic repetitive control of an active filter under varying network frequency: a small-gain theorem-based stability analysis," in *Proceedings of the American Control Conference (ACC), Baltimore, Maryland, USA, 2010*, pp. 1749-1754.
- [12] T.-C. Tsao, Y. X. Qian, and M. Nemani, "Repetitive Control for Asymptotic Tracking of Periodic Signals With an Unknown Period," *Journal of Dynamic Systems Measurement & Control*, vol. 122, pp. 364-369, 2000.
- [13] M. Steinbuch, "Repetitive control for systems with uncertain period-time," *Automatica*, vol. 38, pp. 2103-2109, 2002.
- [14] T. Inoue, "Practical repetitive control system design," in *Decision and Control, Proceedings of the 29th IEEE Conference on, Honolulu, HI, 1990*, pp. 1673-1678.
- [15] R. Costa-Castelló, G. A. Ramos, J. M. Olm, and M. Steinbuch, "Second-order odd-harmonic repetitive control and its application to active filter control," in *Decision and Control (CDC), 2010 IEEE 49th Conference on, Atlanta, Georgia, USA, 2010*, pp. 6967-6972.
- [16] R. Griño and R. Costa-Castelló, "Digital repetitive plug-in controller for odd-harmonic periodic references and disturbances," *Automatica*, vol. 41, pp. 153-157, 2005.
- [17] J. Na, X. Ren, R. Costa-Castelló, and Y. Guo, "Repetitive control of servo systems with time delays," *Robotics and Autonomous Systems*, vol. 62, pp. 319-329, 2014.
- [18] J. Na, R. Griño, R. Costa-Castelló, X. Ren, and Q. Chen, "Repetitive controller for time-delay systems based on disturbance observer," *IET Control Theory & Applications*, vol. 4, pp. 2391-2404, 2010.
- [19] R. Yi and C. Boshi, "Electric drive automatic control system-Motion control system," ed: Beijing, China Machine Press, 2009, pp. 70-71.
- [20] B. A. Francis and W. M. Wonham, "The Internal Model Principle of Control Theory," *Automatica*, vol. 12, pp. 457-465, 1976.
- [21] J. E. Normey-Rico and E. F. Camacho, "Dead-time compensators: A survey," *Control Engineering Practice*, vol. 16, pp. 407-428, 2008.